Optimization of fluorescence enhancement for silicon-based microarrays

Vanessa Marino
University of Palermo
Dipartimento di Ingegneria Elettrica, Elettronica e delle Telecomunicazioni
Viale delle Scienze, edif. 9
Palermo, I-90128, Italy

Clelia Galati
IMS—R&D
STMicroelectronics
Stradale Primosole 50
Catania, I-95121, Italy

Claudio Arnone
University of Palermo
Dipartimento di Ingegneria Elettrica, Elettronica e delle Telecomunicazioni
Viale delle Scienze, edif. 9
Palermo, I-90128, Italy

Abstract. An optical technique for the enhancement of fluorescence detection sensitivity on planar samples is presented. Such a technique is based on the simultaneous optimization of excitation and light collection by properly combining interference and reflectance from the sample holder. Comparative tests have been performed in microarray applications, by evaluating the proposed solution against commercial glass-based devices, using popular labeling dyes, such as Cy3 and Cy5. The proposed technique is implemented on a substrate built with standard silicon technology and is therefore well suited for integrated micro total analysis systems (μTAS) applications. [DOI: 10.1117/1.2992142]

Keywords: fluorescence enhancement; interference; microarray; aluminium-silicon-copper alloy; μTAS.

Paper 08088R received Mar. 13, 2008; revised manuscript received Jun. 27, 2008; accepted for publication Aug. 5, 2008; published online Oct. 9, 2008.

1 Introduction

Fluorescence analysis is a powerful method for research and diagnostics on biological samples and is traditionally applied to measurements on single samples, combined with surface scanning and mapping. A recent development of this method concerns the analysis of microarrays. These consist of a solid planar support that incorporates a two-dimensional array of probes for biochemical assays. Thanks to their miniaturization, they allow simultaneous genomic or proteomic analysis in research applications as well as specialized diagnostics in routine screening applications.[1]

Optical fluorescence detection from microarray spots is now an established laboratory technique due to its high sensitivity and the possibility of labeling a wide range of biomolecules while working on extremely small sample volumes. In DNA microarray analysis, for example, a collection of fluorescent spots is attached to a conventional glass slide for microscopy, each spot being related to a specific level of gene expression. An optical readout system reveals the presence of each spot and the related luminescence intensity, which is related to the concentration of the biological sample in the spot.

Figure 1 refers to a typical commercial confocal array scanning system. A laser source illuminates the microarray slide positioned on an *XY* scanning stage, and a photomultiplier collects the filtered fluorescence light from the slide surface. The laser beam has a wavelength as close as possible to the dye maximum absorption wavelength. Emission detection is based on a combination of confocal spatial filtering and spectral selectivity. The confocal structure removes most stray light from out-of-focus planes. Spectral filtering optimizes the rejection of the laser wavelength through a sharp cutoff filter in front of the detector.

In an ideal system, only the fluorescence generated from the sample should be collected. In a real scanner, the emitted fluorescence signal is affected by a background noise. A number of sources contribute to this noise: unfiltered specular or diffuse reflection of the laser light from the labeled sample, autofluorescence of the substrate supporting the microarray, autofluorescence from contaminants on the surface and from the optical imaging system, stray light, and dark current of the photomultiplier.

High sensitivity detection in microarray systems is often a challenge for the extremely small fluorescence volumes that could be involved. For example, rare levels of gene or protein expressions are related to very small concentrations of labeled molecules, providing low signal levels. If the collected fluorescence signal is comparable with the background signals and detector noise, then no useful information can be obtained from the array.

Besides an accurate control of all noise sources, the optical properties of the array substrate have a main influence on the measurement sensitivity. A number of efforts have been made for improving this parameter by designing dedicated surfaces for the array.[2] The sensitivity can be enhanced by increasing the hybridization yield[3] or by enabling a higher binding capacity through the use of porous surfaces[4,5] and silicon nanostructures.[6] Other possibilities concern the enhancement of luminescence capture efficiency through the modification of the surface layout, creating local mechanical sites for the spots.[7]

The collected fluorescence can be also amplified by covering the substrate with a reflective film[8] or exploiting an optical

Address all correspondence to Claudio Arnone, Dipartimento di Ingegneria Elettrica, Elettronica e delle Telecomunicazioni, University of Palermo, Viale delle Scienze, edif. 9, I-90128 Palermo, Italy; Tel.: 39–091–6615278; Fax: 39–091–488452; e-mail: arnone@unipa.it

1083-3668/2008/13(5)/054060/6/$25.00 © 2008 SPIE

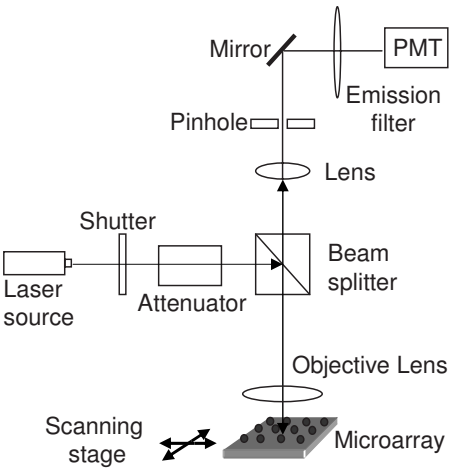

Fig. 1 Simplified optical setup of a confocal single-channel scanning system for microarray analysis.

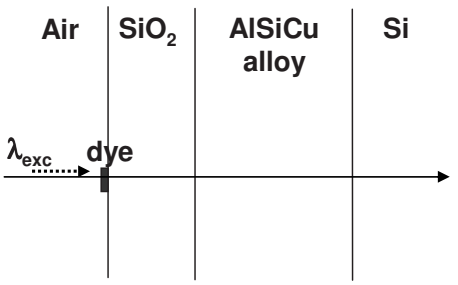

Fig. 2 Structure of the OMS substrate.

constructive interference created by the substrate. To this purpose, several solutions have been proposed, involving coating of glass substrates with dielectric or metal films[9–11] or the use of silicon planar reflectors covered with a thin film of silicon dioxide.[12,13]

The solution presented here is based on the simple two-layer reflector shown in Fig. 2. This platform is made of a silicon substrate covered with a reflective film of aluminum-silicon-copper alloy and a second layer of silicon dioxide. This oxide-metal-silicon (OMS) structure is all made with standard materials used in modern silicon processing for microelectronics. The aluminum-based alloy is commonly used for metal interconnects in integrated circuits. In the visible spectrum, it exhibits high reflectance and absence of autofluorescence. This metallized silicon surface is used as an optical reflector for the fluorescence signal, allowing collection of most of the fluorescence that would otherwise be scattered and lost toward the substrate.

The SiO_2 layer acts as a spacer between the mirror and the fluorescent material. It has a relevant role in maximizing the measured signal because its thickness optimizes, by interference, the optical excitation of the fluorescent labels. By properly sizing the oxide thickness, the maximum electric field of the laser electromagnetic wave can be allocated exactly on the surface, that is on the labeled biomaterial.

In order to estimate the optimized oxide thickness for maximum fluorescence collection in OMS structures, we used a direct electromagnetic simulation. The collected fluorescence intensity was computed as a function of the oxide thickness, for biological molecules labeled with Cy3 or Cy5 fluorescent cyanine dyes and at normal incidence. For the experimental tests, a set of wafers coated with SiO_2 was prepared. Tests have been performed by using Cy3 and Cy5 labels on both the OMS substrate and commercial glass-based slides.

2 Theoretical Modeling

Both incident and emitted light independently interfere with their reflection from the mirror. This is possible because the absorption of the thin oxide layer is negligible and the small bandwidth of both laser and fluorescence light results in a coherence length well above the oxide thickness. When dealing with the theoretical aspects of fluorescence optimization by interference, two different approaches can be found in the literature. On one side, only interference at the excitation wavelength is considered, maximizing the laser electric field at the sample surface. On the other side, a more complex approach is followed, according to the theory first exposed by Lambacher and Fromherz[14] and further developed by Parthasarathy and Groves.[15] In this case, the collected fluorescence (I) is proportional to the product of the excitation probability per unit time (P_{exc}) and the probability of capturing an emitted photon per unit time (P_{em}),

$$I \cap P_{ex} \cdot P_{em} \cap [(1-r_{ex})^2 + 4r_{ex}\sin^2(\phi_{in}/2)][(1-r_{em})^2 + 4r_{em}\sin^2(\phi_{out}/2)], \quad (1)$$

where φ_{in} and φ_{out} indicate the phase difference between incident and reflected fields, and r_{ex}, r_{em} are the Fresnel reflection coefficients, respectively, for the excitation and emission wavelength.

The SiO_2 thickness design reported here is made according to the first approach, which is considering only interference at the laser wavelength. The involvement of the second approach in the OMS performances is considered in the final discussion on the results.

The thickness of the spacer and the alloy layer, as well as the complex refractive index of the alloy, all contribute to the optimal phase condition of the electromagnetic field in the oxide layer. Because of attenuation inside the metal film, this can be considered of infinite extension, as the transmitted energy is fully absorbed in a layer of <100 nm. This is the case for the metal thickness values used here, indicated in Section 3. Hence, the laser electromagnetic field becomes negligible before reaching the silicon substrate, which therefore has no effect on the model, acting only as a quality mechanical support. The incident and reflected waves are supposed to be normal to the surface, and the phase contribution of the surface functionalization layer and oligonucleotide probes is neglected because they are typically a few nanometers thick.

For optimal light absorption, a maximum of the excitation electric field must be positioned on the probe plane. This is obtained by adding in phase the field of the incoming laser light (E^+) and its reflection (E^-) from the mirror surface, with $|E^-| \approx |E^+|$. With this condition, a fourfold light power increase occurs, as this is proportional to the square of the total field, with $(E^- + E^+)^2 \approx (2E^+)^2$.

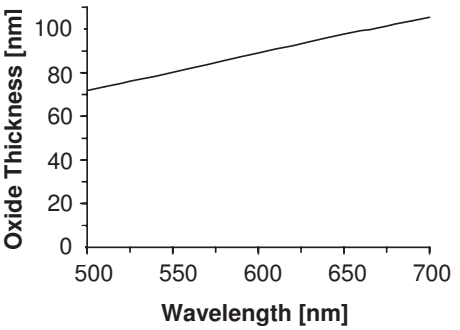

Fig. 3 Optimal oxide thickness versus excitation wavelength (normal incidence) for the OMS structure.

The lossless oxide layer contains a standing wave due to the interference between E^+ and E^-. The total field at the OMS surface results,

$$E = E^+ + E^- = E^+[1 + |\rho| e^{j\delta_0} e^{2jkd}], \quad (2)$$

where $k = 2\pi n_{ox}/\lambda_0$ at the excitation wavelength, d is the oxide thickness, and $\rho = |\rho| e^{j\delta_0}$ is the reflection coefficient for the electric field at the oxide-metal interface. The phase shift δ_0 accounts for the complex refractive index of the metal layer. Both δ_0 and kd determine the position of the maxima of the standing wave.

By using a sufficiently thin oxide film, the standing wave has only one maximum, which we place on the OMS surface. According to (2), the electric field is maximum when the term $e^{j\delta_0} e^{2jkd}$ is real and the magnitude of the field is then proportional to $1 + |\rho|$. This condition was evaluated by the Essential Macleod optical design software.[16] Figure 3 shows the optimal oxide thickness as a function of the excitation wavelength.

With reference to typical excitation wavelengths for Cy3 and Cy5, a complex index of $\tilde{n} = 1.21 - j6.92$ for 633 nm and $\tilde{n} = 0.81 - j5.96$ for 543 nm was used for the metal film. For the oxide, $n_{ox} = 1.457$ for 633 nm and $n_{ox} = 1.460$ for 543 nm were assumed. It should be noted that the optimal thickness does not correspond to $\lambda/4$ due to the phase shift introduced by the lossy metal film.

With reference to Cy3 ($\lambda_{exc} = 543$ nm) and Cy5 ($\lambda_{exc} = 633$ nm) fluorescent dyes, these simulations showed that the optimal thickness values are respectively 79 and 95 nm. The computed electric field profiles in the OMS structure for these two specific situations are shown in Figs. 4(a) and 4(b)

It is interesting to observe that a slight "detuning" of the oxide film does not compromise an efficient excitation, and it results profitable when the same OMS device is used for both dyes. For example, Fig. 4(c) shows the electric field distribution in a detuned film, where the 95 nm oxide thickness, optimal for Cy5, is used at the Cy3 excitation wavelength.

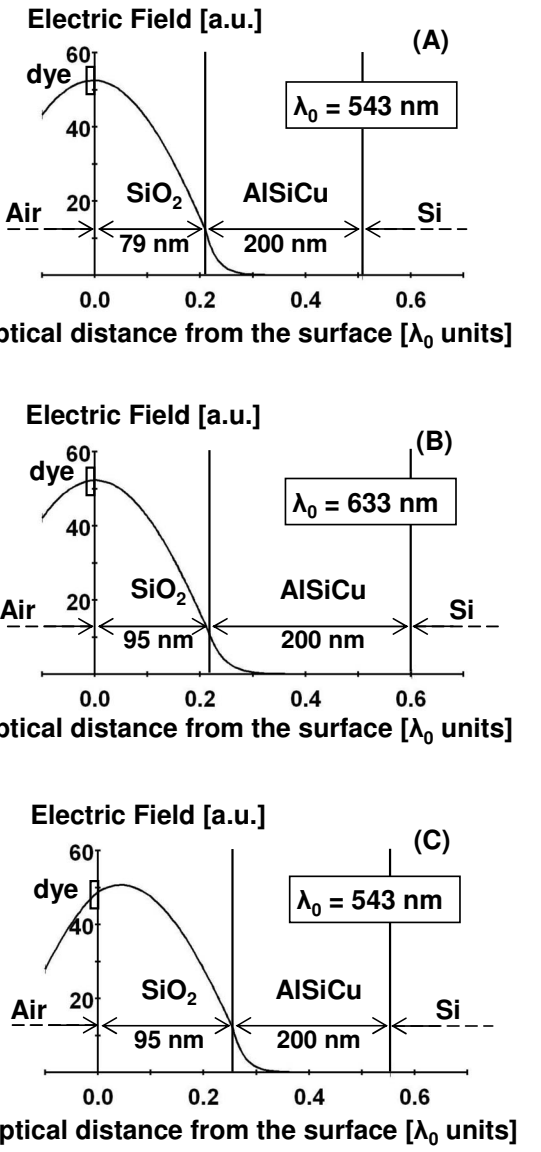

Fig. 4 Electric field distribution on the OMS structure for normal incidence: (A) Cy3 excitation at 543 nm, (B) Cy5 excitation at 633 nm, and (C) Cy3 excitation in an oxide film optimized for Cy5.

3 Sample Preparation

In order to test the theoretical results, three sets of 6-in. silicon wafers were prepared using standard silicon processing steps. One set was covered with a 200-nm film of sputtered aluminum-silicon-copper alloy (1 wt % silicon and 0.5 wt % copper in aluminum). A second set was coated with a 1000-nm alloy film. A third set was not metallized at all, in order to evaluate the role of surface smoothness on the detected signal, as discussed later.

Next, an oxide film with a thickness of 95 nm—optimized for Cy5—was deposited on all wafers, using a plasma-enhanced chemical vapor deposition process in an Applied Materials 5000-2 system. An accurate verification of the thickness of the oxide film was made by a Sentech 850 ellipsometer.

From each wafer, seven 1×3 in. slides were cut, according to the size of common glass slides for microscopy. This size allowed further processing through standard spotting equipment, as well as analysis of the samples through an array scanning system.

Silanization, which is the surface chemical modification for immobilizing the biomolecules on the substrate, was the next step. In order to obtain uniform and reproducible surface

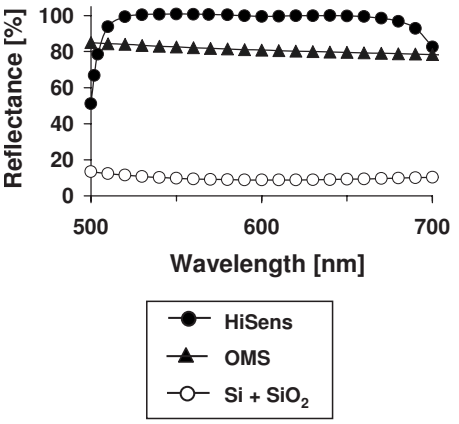

Fig. 5 Comparison of total reflectance measurements performed on OMS, Nexterion HiSens and oxidized silicon slides.

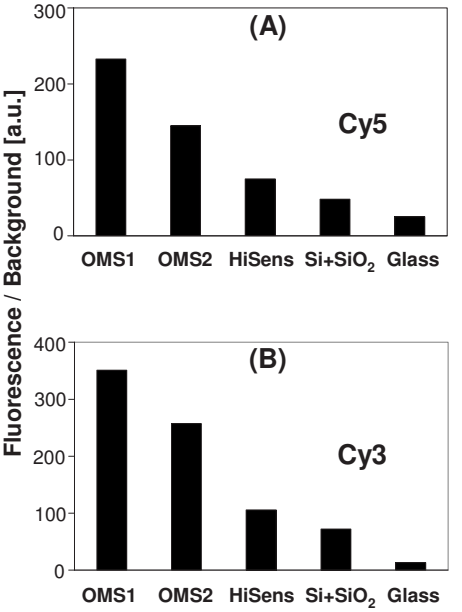

Fig. 6 (A) Array scanning measurements, respectively, on OMS, HiSens E, oxidized silicon, and glass slides for Cy5 (Perkin Elmer ScanArray). OMS1 refers to samples with a 200-nm-thick AlSiCu film, and OMS2 refers to a 1000-nm film. In OMS and silicon samples, the oxide thickness is 95 nm. (B) Same substrates as (A), with Cy3 matching excitation.

conditions, water adsorption and particle microcontamination had to be minimized during this critical step. This was achieved by preparing the surface in a glove box pressurized with high-purity inert gas, such as nitrogen or argon. Standard RCA cleaning was made first.[17] Next, an oxidizing acid wash was used for removing carbon contamination and increasing the number of reactive hydroxyl groups by breaking syloxane bonds on the oxide surface. After this pretreatment, the slides were immersed for 4 h in a room-temperature solution of sylane reagent molecules (3-glycidoxypropyltriethoxysilane) in toluene.[18] Rinsing in toluene and blow-drying with N_2 followed.

The fluorescent probes were obtained from a 23-mer 5′-amine modified oligonucleotide, labeled with Cy5 and dissolved in sodium phosphate buffer with 9.3 pH. The resulting 5-μM oligonucleotide solution was spotted on the silanized slides as a 16×16 spot array, by a noncontact piezodriven microdispensing system (Piezorray™ by Perkin Elmer). The same procedure was followed for Cy3-labeled oligonucleotides. The 5-μM concentration value was chosen for a good fluorescence visibility on the glass slides used as a reference for the measurements. All spotted slides were stored in a sealed chamber containing a saturated NaCl solution in order to keep a constant humidity environment around 75%.[19] This incubation was carried out overnight, at room temperature. Rinsing and drying followed according to standard procedures.[20]

In order to perform comparative measurements, a bare glass slide and a commercial high-sensitivity slide (Nexterion® HiSens E) were also processed in the same way.

4 Experimental Results and Discussion

To the authors' knowledge, the use of the proposed OMS structure as a high-reflectance layer for fluorescence enhancement has not been reported before. The OMS performances are discussed here in terms of morphological and optical characterization for microarray application.

Substrate total reflectance was tested before biofunctionalization and spotting, using a Perkin Elmer Lambda 900 spectrophotometer, in the 500–700 nm range. This measurement (Fig. 5) showed that wafers with different thicknesses of the metal film (200 and 1000 nm) exhibit the same total (specular and diffused) reflectance. Figure 5 reports also the reflectance measurement for the Nexterion HiSens E glass-based slide and for the oxidized silicon sample. As expected, the commercial sample exhibits practically 100% reflectivity because it is designed for this purpose. The OMS slide has a reduced 80% total reflectance over the whole 500–700 nm range. This is due to the oxide film, whose thickness makes up an antireflection layer. The same effect can be observed for the oxidized silicon sample, where the natural reflectivity of the silicon surface (~40%) is reduced to nearly 10%. These measurements are of special interest: even if the oxide layer reduces the metal reflectivity (normally around 90%), this remains quite high, due to the metal itself. But the oxide layer creates a maximum in the surface electric field, optimizing dye excitation. The same cannot be stated for oxidized silicon: in this case, even if the oxide thickness is close to the optimal value for maximizing the surface field—as separately computed with Essential Macleod—the resulting reflectivity is too poor if compared to the metallized sample.

Next, tests with microarrays deposited on the samples where performed using a ScanArray Express (PerkinElmer). The substrates with 200- and 1000-nm-thick reflectors were compared to Nexterion HiSens slides, with oxidized silicon and with bare glass. Figure 6(a) shows the ratio of the collected fluorescence to background signal for Cy5 labels, computed as (fluorescence—noise)/noise. The fluorescence intensity was computed by averaging the signal collected from 32 spots, and the noise was evaluated in unspotted areas far from fluorescent spots. A sensitivity enhancement in OMS substrates with 200-nm metal layer was observed by a factor averaged around 3, 5, and 9 compared, respectively, to the HiSens slide, the oxidized silicon, and the glass slide. A

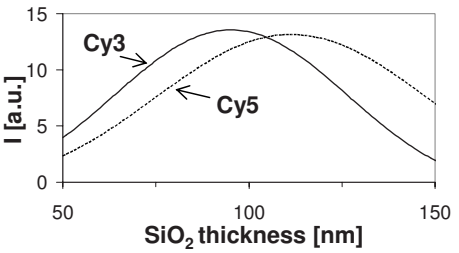

Fig. 7 Computed fluorescence signal from the OMS as a function of oxide layer thickness, according to Parthasarathy and Groves model.[15]

smaller factor resulted from OMS samples with a 1000-nm reflector.

According to the plots in Figs. 3 and 4(c), the oxide thickness optimized for Cy5 is not too far from to the optimal thickness for Cy3. Hence, a test was made by measuring the fluorescence to background signal for Cy3 using the oxide optimized for Cy5. Figure 6(b) shows the results of this experiment with a fluorescence enhancement comparable to that of Fig. 6(a). This result shows that an OMS structure calculated for Cy5 is sufficiently noncritical for producing a good enhancement also for Cy3. This result can be explained in terms of Eq. (1). According to such a model, a thickness of 95 nm is optimal for the Cy3, with excitation at 543 nm and fluorescence collection at 570 nm (Fig. 7). Further discussion on the best theoretical approach to follow for the OMS structure is not in the aim of this work but, whichever the theoretical approach is, the experimental results clearly indicate that the OMS substrate with 95-nm-thick oxide is a fairly good substrate for both Cy3 and Cy5 dyes.

It is worth evidencing that the enhancement ratio between HiSens slides and bare glass is compatible with Nexterion published results.[9] However, the improvement given by the OMS structure against the commercial slide requires further comments or speculations. The commercial slide exhibits 100% reflectivity, obtained through a multilayer dielectric stack made of more than 15 layers. The field distribution in a complex dielectric stack (i.e., the position of nodes and antinodes, as well as the period of the standing wave) critically depends on the optical thickness of each layer, including the upper surface medium. Consequently, small changes in the index of this medium may lead to a loss of resonance in the whole stack. For this reason, the value of the electric field on the surface of the multidielectric slide has a more critical dependence on thickness and refractive index of the surface functionalization and the analyte films. This may easily result in an excitation field whose value is not maximum at the surface. Conversely, the OMS substrate, with its simple optical structure, is capable of keeping on the surface the maximum of the electric field in a more relaxed way, making it not very sensitive to surface layers.

A final discussion is related to the morphology of the reflecting structure. The OMS uses a sputtered metal reflector, with some amount of surface roughness. This increases with the layer thickness and is originated by the sputtering process used for its deposition.[21]

Figure 8 reports the surface topographical measurements performed on three different samples after the cleaning process and before silanization. The measurements were made by a PSIA XE-150™ atomic force microscopy in "true noncontact" mode on a 50×50 μm area. The slide with the 1000-nm alloy exhibits a root-mean-square roughness of $\sim$25 nm. This value is reduced to $\sim$7 nm with a 200-nm-thick alloy, and to 0.3 nm with no film at all. This reduction was also qualitatively confirmed by simple optical measurements, performed by illuminating the samples with a 633-nm laser beam and evaluating the intensity of the diffused reflection, after removing the specular reflection with an optical stop. Such tests also indicated that the oxide layer has practically no role in determining the final roughness.

To the authors' opinion, the surface microroughness can affect the amplitude of the collected fluorescence signal. The optimal roughness value should be set according to the structure of the collection optics in the array scanner. In a typical scanning system, such as the ScanArray Express, for example, the optical readout system of the instrument is capable to reject almost completely the specular reflection from the sample while collecting the diffused luminescence.[22] Because the aperture of the collection optics is limited, the angular distribution of backscattered fluorescence, which is directly correlated to surface roughness, should match the aperture itself, maximizing signal collection. In this view, the results shown in Fig. 6 suggest that the OMS1, with lower roughness

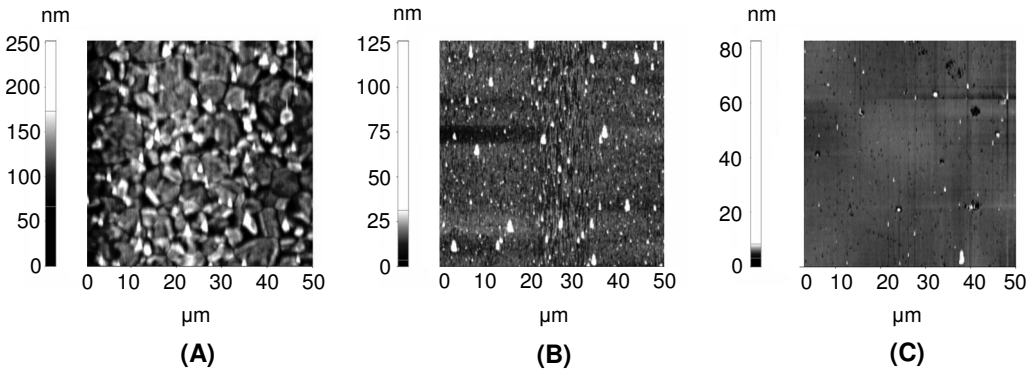

Fig. 8 AFM morphological analysis: (A) 1000-nm aluminum alloy film covered with 95 nm SiO_2, with rms roughness of 25 nm; (B) 200-nm aluminum alloy film and 95 nm SiO_2, with rms roughness of 7 nm; and (C) silicon reference sample, coated with a 95-nm SiO_2 film. The rms roughness is 0.3 nm.

(that is with thinner metal film), was better matched with the collection optics of the reader. This may also explain the better performances of the OMS structure against the ultrasmooth commercial slides.

Conclusions

We designed and tested an optical structure capable to enhance the fluorescence collection from planar biological samples. Even if, in principle, this structure can be implemented on any planar surface, here it is referred to standard and low-cost silicon technology and is mainly proposed for applications in array scanning systems.

The key feature of this OMS structure is the possibility of maximizing the fluorescence excitation of the samples without significantly compromising the substrate reflectivity. In comparison to traditional glass slides or other commercial substrates, the improved fluorescence collection obtained with the OMS substrate allows a better quantitative analysis, thanks to a greatly increased signal-to-noise ratio at the detector.

Practical tests of the OMS structure were made on microarrays of Cy3 and Cy5 labeled oligonucleotides. The achieved results confirmed the theoretical predictions and their well competing behavior against other substrates proposed in the literature or commercially available.

Besides the application in microarrays, the design guideline followed for the OMS substrate can be used in other areas of biophotonics, such as tissue and living cell fluorescence imaging. Moreover, the full compatibility with standard silicon processing makes the OMS substrate a good candidate for μTAS applications or other silicon based optical sensors for biomedical research and clinical diagnostics.

Acknowledgments

We thank Professor Angus Macleod of the University of Arizona for his suggestions and his precious help and Dr. Salvatore Coffa of STMicroelectronics for suggesting and encouraging this work.

References

1. T. Vo-Dinh, "Biochips and microarrays: Tools for the new medicine," in *Biomedical Photonics Handbook*, T. Vo-Dinh, Ed., SPIE, Bellingham, WA, (2003).
2. W. Kusnezow and J. D. Hoheisel, "Solid supports for microarray immunoassays," *J. Mol. Recognit.* **16**, 165–176 (2003).
3. S. Taylor, S. Smith, B. Windle, and A. Guiseppi-Elie, "Impact of surface chemistry and blocking strategies on DNA microarrays," *Nucleic Acids Res.* **31**(16), e87 (2003).
4. F. Bessueille, V. Dugas, V. Vikulov, J. P. Cloarec, E. Souteyrand, and J. R. Martin, "Assessment of porous silicon substrate for well-characterised sensitive DNA chip implement," *Biosens. Bioelectron.* **21**, 908–916 (2005).
5. D. Proudnikov, E. Timofeev, and A. Mirzabekov, "Immobilization of DNA in polyacrylamide gel for the manufacture of DNA and DNA-oligonucleotide microchips," *Anal. Biochem.* **259**, 34–41 (1998).
6. C. Oillic, P. Mur, E. Blanquet, G. Delapierre, F. Vinet, and T. Billon, "DNA microarrays on silicon nanostructures: optimization of the multilayer stack for fluorescence detection," *Biosens. Bioelectron.* **22**, 2086–2092 (2007).
7. R. Blue, N. Kent, L. Polerecky, H. McEvoy, D. Gray, and B. D. MacCraith, "Platform for enhanced detection efficiency in luminescence-based sensors," *Electron. Lett.* **41**(12), 682–684 (2005).
8. E. Le Moal, E. Fort, S. Léve Que-Fort, A. J. H. Murata, F. P. Cordelières, M. P. Fontaine-Aupart, and C. Ricolleau, "Mirror slides for high-sensitivity cell and tissue fluorescence imaging," *J. Biomed. Opt.* **12**(2), 024030(2007).
9. R. J. Redkar, N. A. Schultz, V. Scheumann, L. A. Burzio, D. E. Haines, E. Metwalli, O. Becker, and S. D. Conzone, "Signal and sensitivity enhancement through optical interference coating for DNA and protein microarray applications," *J. Biomol. Tech.* **17**(2), 122–130 (2006).
10. B. Fouquè, B. Schaack, P. Obeid, S. Combe, S. Getìn, P. Barritault, P. Chaton, and F. Chatelain, "Multiple wavelength fluorescent enhancement on glass substrates for biochip and cell analysis," *Biosens. Bioelectron.* **20**, 2335–2340 (2005).
11. H. Choumane, N. Ha, C. Nelep, A. Chardon, G. O. Reymond, C. Goutel, G. Cerovic, F. Vallet, and C. Weisbuch, "Double interference fluorescence enhancement from reflective slides: application to bicolor microarrays," *Appl. Phys. Lett.* **87**, 031102(2005).
12. J.-N. Volle, G. Chambon, A. Sayah, C. Reymond, N. Fasel, and M. A. M. Gijs, "Enhanced sensitivity detection of protein immobilization by fluorescent interference on oxidized silicon," *Biosens. Bioelectron.* **19**, 457–464 (2003).
13. M. Bras, V. Dugas, F. Bessueille, J. P. Cloarec, J. R. Martin, M. Cabrera, J. P. Chauvet, E. Souteyrand, and M. Garrigues, "Optimisation of a silicon/silicon dioxide substrate for a fluorescence DNA microarray," *Biosens. Bioelectron.* **20**, 797–806 (2004).
14. A. Lambacher and P. Fromherz, "Fluorescence interference-contrast microscopy on oxidized silicon using a monomolecular dye layer," *Appl. Phys. A* **63**, 207–216 (1996).
15. R. Parthasarathy and J. T. Groves, "Optical techniques for imaging membrane topography," *Cell Biochem. Biophys.* **41**(3), 391–414 (2004).
16. *Thin Film Center, The Essential Macleod*, version 8.14, Thin Film Center Inc., Tucson (1995–2007).
17. W. Kern, "The evolution of silicon wafer cleaning technology," *J. Electrochem. Soc.* **137**(6), 1887–1892 (1990).
18. P. E. Lobert, D. Bourgeois, R. Pampin, A. Akheyar, L. M. Hagelsieb, D. Flandre, and J. Remacle, "Immobilization of DNA on CMOS compatible materials," *Sens. Actuators B* **92**, 90–97 (2003).
19. F. E. M. O'Brien, "The control of humidity by saturated salt solutions," *J. Sci. Instrum.* **25**, 73–76 (1948).
20. M. Vigano, R. Suriano, M. Levi, S. Turri, M. Chiari, and F. Damin, "Glass silanization with blocked-isocyanate for the fabrication of DNA microarrays," *Surf. Sci.* **601**, 1365–1370 (2007).
21. S. Bader, E. M. Kalaugher, and E. Arzt, "Comparison of mechanical properties and microstructure of Al (1 wt.%Si) and Al (1 wt.%Si, 0.5 wt.%Cu) thin films," *Thin Solid Films* **263**, 175–184 (1995).
22. A. Osgood and M. Schermer, "Imaging system for an optical scanner," U.S. Patent No. 6,441,379 B1 (2002).